

Accepted Article

Title: Towards an Understanding of Halide Interactions with the Carbonyl-Containing Molecule CH₃CHO

Authors: Timothy Robert Corkish, Christian Thrane Haakansson, Peter Daniel Watson, Hayden Thomas Robinson, Allan James McKinley, and Duncan Andrew Wild

This manuscript has been accepted after peer review and appears as an Accepted Article online prior to editing, proofing, and formal publication of the final Version of Record (VoR). This work is currently citable by using the Digital Object Identifier (DOI) given below. The VoR will be published online in Early View as soon as possible and may be different to this Accepted Article as a result of editing. Readers should obtain the VoR from the journal website shown below when it is published to ensure accuracy of information. The authors are responsible for the content of this Accepted Article.

To be cited as: *ChemPhysChem* 10.1002/cphc.202100180

Link to VoR: <https://doi.org/10.1002/cphc.202100180>

COMMUNICATION

Towards an Understanding of Halide Interactions with the Carbonyl-Containing Molecule CH₃CHO

Timothy R. Corkish,^[a] Christian T. Haakansson,^[a] Peter D. Watson,^[a] Hayden T. Robinson,^[a] Allan J. McKinley^[a] and Duncan A. Wild*^[a]

[a] T. R. Corkish, C. T. Haakansson, P. D. Watson, H. T. Robinson, Prof. A. J. McKinley, Dr. D. A. Wild
School of Molecular Sciences
The University of Western Australia
Crawley, Western Australia, 6009, Australia
E-mail: duncan.wild@uwa.edu.au

Supporting information for this article is given via a link at the end of the document.

Abstract: The anion photoelectron spectra of Cl⁻⋯CD₃CDO, Cl⁻⋯(CD₃CDO)₂, Br⁻⋯CH₃CHO, and I⁻⋯CH₃CHO are presented with respective electron stabilisation energies of 0.55 eV, 0.93 eV, 0.48 eV, and 0.40 eV. Optimised geometries of the singly solvated species featured the halide appended to the CH₃CHO molecule in-line with the electropositive portion of the C=O bond and have binding energies between 45 and 52 kJ mol⁻¹. The doubly solvated Cl⁻⋯(CH₃CHO)₂ species features asymmetric solvation upon the addition of a second CH₃CHO molecule. Theoretical detachment energies were found to be in excellent agreement with experiment, with comparisons drawn between other halide complexes with simple carbonyl molecules.

Determining the nature of ion solvation and ion-molecule interactions lies at the heart of experimental anion photoelectron spectroscopy. In mass selecting a cluster size for interrogation, one can investigate molecular structure and the stepwise solvation of an anion as it transitions from the gas phase to more solution-based contexts.^[1,2]

Landmark work in the field by Markovich has centered on halide anion solvation in the gas phase by up to 60 water molecules, simulating solvent effects.^[3-5] The photodetachment of an electron associated with the halide anion exhibits a 'solvent shift', known as the electron stabilisation energy, E_{stab} , which increases further upon subsequent solvation, retaining the detachment profile of the bare halide anion.^[6] This solvent shift is largely dependent on the strength of the interaction between the halide anion and complexing neutral molecule.^[7] Our group has recently combined anion photoelectron spectroscopy and CCSD(T) calculations to probe the electronic structure of systems involving halogen bonding,^[8] as well as ion-radical^[9] and ion-multipole^[10] interactions.

An interesting facet of gas-phase solvation emerges when moving beyond a singly solvated system, known as asymmetric solvation. That is, in cases such as X⁻⋯(H₂O)₂, where X = Cl, Br, I, the lowest energy configuration of the system involves the two H₂O molecules positioned at the same face of the anion, one donating two hydrogen bonds and the other acting simultaneously as hydrogen bond donor and acceptor.^[11,12]

This binding motif is also present for diatomic anion species,^[13,14] as well as for other solvent molecules, such as CH₃OH.^[15] Asymmetric solvation can then provide an insight to species that preferentially undergo surface solvation.

Attention in this work is turned towards the CH₃CHO molecule: among the most abundant atmospheric carbonyl molecules, produced photochemically as well as through motor vehicle exhaust.^[16-19] The reaction between Br + CH₃CHO reduces the

chain length of catalytic O₃ destruction in the Arctic marine boundary layer,^[20] and with a general focus or outcome pertaining to the hydrogen abstraction channel, neutral halogen reactions with CH₃CHO have been widely studied.^[21-36]

Anion photoelectron spectroscopy is well known for its ability to access the energetics of a transient neutral state through the more stable anion counterpart, with vibrational resolution achievable with higher resolution approaches.^[2]

This work will present the anion photoelectron spectra of Cl⁻⋯CD₃CDO, Cl⁻⋯(CD₃CDO)₂, Br⁻⋯CH₃CHO, and I⁻⋯CH₃CHO in order to provide fundamental information about these systems including E_{stab} energies, especially pertinent to the stepwise solvation of Cl⁻. Computational work is presented to complement the experimental results, with geometries and predicted detachment energies used to rationalise the electronic structure. Furthermore, the results will be compared to previous studies involving CH₂O^[37] and CH₃COCH₃^[38] in order to establish general trends observed for halide-carbonyl molecule systems.

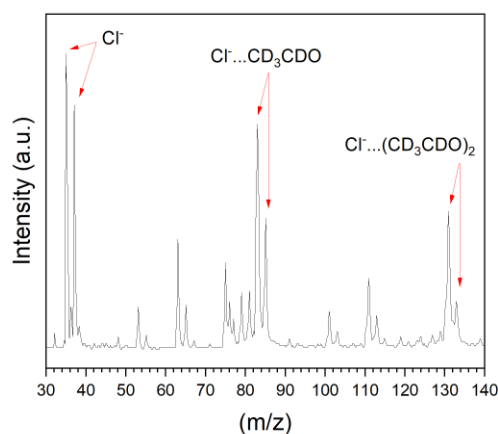


Figure 1. A negative ion mass spectrum of a gas mixture containing CCl₄, CD₃CDO, and Ar.

Figure 1 shows a representative negative ion mass spectrum of a gas mixture consisting of CCl₄, CD₃CDO, and Ar. CD₃CDO was chosen for Cl⁻ experiments to avoid a potential mass contamination involving Br⁻ and Cl⁻⋯CH₃CHO (79 m/z and 81 m/z). The deuteration of CD₃CDO is expected to result in a minimal difference in the photoelectron spectrum of Cl⁻⋯CD₃CDO relative to Cl⁻⋯CH₃CHO, as will be shown later through predicted CCSD(T) detachment energies for both species.

COMMUNICATION

Labelled in the mass spectrum are the isotopes of the Cl^- anion (35 m/z and 37 m/z), the $\text{Cl}^- \cdots \text{CD}_3\text{CDO}$ complex (83 m/z and 85 m/z), and the $\text{Cl}^- \cdots (\text{CD}_3\text{CDO})_2$ complex (131 m/z and 133 m/z). Br^- anion mass peaks at 79 m/z and 81 m/z are present in this spectrum as remnants from a previous experiment. Other significant mass peaks include $\text{Cl}^- \cdots \text{H}_2\text{O}$ (53 m/z and 55 m/z), $\text{Cl}^- \cdots \text{N}_2$ (63 m/z and 65 m/z), $\text{Cl}^- \cdots \text{Ar}$ (75 m/z and 77 m/z), $\text{Cl}^- \cdots \text{H}_2\text{O} \cdots \text{CD}_3\text{CDO}$ (101 m/z and 103 m/z) and $\text{Cl}^- \cdots \text{N}_2 \cdots \text{CD}_3\text{CDO}$ (111 m/z and 113 m/z).

The anion photoelectron spectra of $\text{Cl}^- \cdots \text{CD}_3\text{CDO}$, $\text{Cl}^- \cdots (\text{CD}_3\text{CDO})_2$, $\text{Br}^- \cdots \text{CH}_3\text{CHO}$, and $\text{I}^- \cdots \text{CH}_3\text{CHO}$ are shown in Figure 2. Additionally, experimental and theoretical ${}^2P_{3/2}$ and ${}^2P_{1/2}$ detachment energies are included in Table 1 along with E_{stab} values, being the difference between the experimental ${}^2P_{3/2}$ energies of the bare halide relative to the complexed halide i.e., Cl^- to $\text{Cl}^- \cdots \text{CD}_3\text{CDO}$.

The $\text{Cl}^- \cdots \text{CD}_3\text{CDO}$ and $\text{Cl}^- \cdots (\text{CD}_3\text{CDO})_2$ anion photoelectron spectra are characterised by a single peak as the neutral ${}^2P_{3/2}$ and ${}^2P_{1/2}$ states are not resolved due to resolution limitations of the apparatus. The respective E_{stab} values for these complexes are 0.55 eV and 0.93 eV, meaning that a valence electron associated with a Cl^- anion is stabilised by a further 0.38 eV upon complexing with a second CD_3CDO molecule.

The $\text{Cl}^- \cdots (\text{CD}_3\text{CDO})_2$ photoelectron spectrum appears narrower for two reasons. Firstly, there is a smaller spread in electron energies as the detached electrons, being close in energy to the laser threshold, have less kinetic energy when detached.^[39] Secondly, there is a small potential for the peak to be cut off by the threshold. CCSD(T) calculations below show the ${}^2P_{1/2}$ detachment peak is predicted on the cusp of laser detachment at 4.66 eV (see Table 1).

Both photoelectron spectra associated with the $\text{Br}^- \cdots \text{CH}_3\text{CHO}$ and $\text{I}^- \cdots \text{CH}_3\text{CHO}$ complexes show resolution of the ${}^2P_{3/2}$ and ${}^2P_{1/2}$ detachment peaks, with the splitting between these peaks indicative of photodetachment from perturbed Br^- and I^- anions. Some disturbance is noted in the $\text{Br}^- \cdots \text{CH}_3\text{CHO}$ photoelectron spectrum prior to the onset of the major ${}^2P_{3/2}$ peak and this is believed to be the result of a background subtraction.

The respective E_{stab} energies for $\text{Br}^- \cdots \text{CH}_3\text{CHO}$ and $\text{I}^- \cdots \text{CH}_3\text{CHO}$ are 0.48 eV and 0.40 eV. Thus, E_{stab} values were observed to increase in the order of $\text{I}^- < \text{Br}^- < \text{Cl}^-$. This trend is to be expected as it follows the order of halide size, with the smallest halide providing the greatest stabilising effect. As will be reiterated later with respect to CCSD(T) detachment energies, the deuteration of $\text{Cl}^- \cdots \text{CD}_3\text{CDO}$ is expected to have a negligible effect on the stabilisation energy, at least for the singly solvated species.

The theoretical detachment energies provided in Table 1 have been derived from CCSD(T)/AVTZ optimised geometries of $\text{Cl}^- \cdots \text{CH}_3\text{CHO}$, $\text{Br}^- \cdots \text{CH}_3\text{CHO}$, and $\text{I}^- \cdots \text{CH}_3\text{CHO}$, where AVTZ = aug-cc-pVTZ for first-row atoms,^[40] aug-cc-pV(T+d)Z for Cl ,^[41] and aug-cc-pVTZ-PP for Br and I .^[42,43] These geometries are presented in Figure 3, along with the DSD-PBEP86/AVTZ optimised geometry of $\text{Cl}^- \cdots (\text{CH}_3\text{CHO})_2$ in Figure 4.

The anion complex geometries all feature a similar binding motif; with the halide interacting with both the formyl and methyl hydrogens of CH_3CHO . The distance to the formyl hydrogen increases from 2.66 Å for Cl^- , to 2.81 Å for Br^- , and 3.07 Å for I^- . A major feature of interest is that the $\text{Br}^- \cdots \text{CH}_3\text{CHO}$ and $\text{I}^- \cdots \text{CH}_3\text{CHO}$ complexes are of C_1 symmetry, with the halide

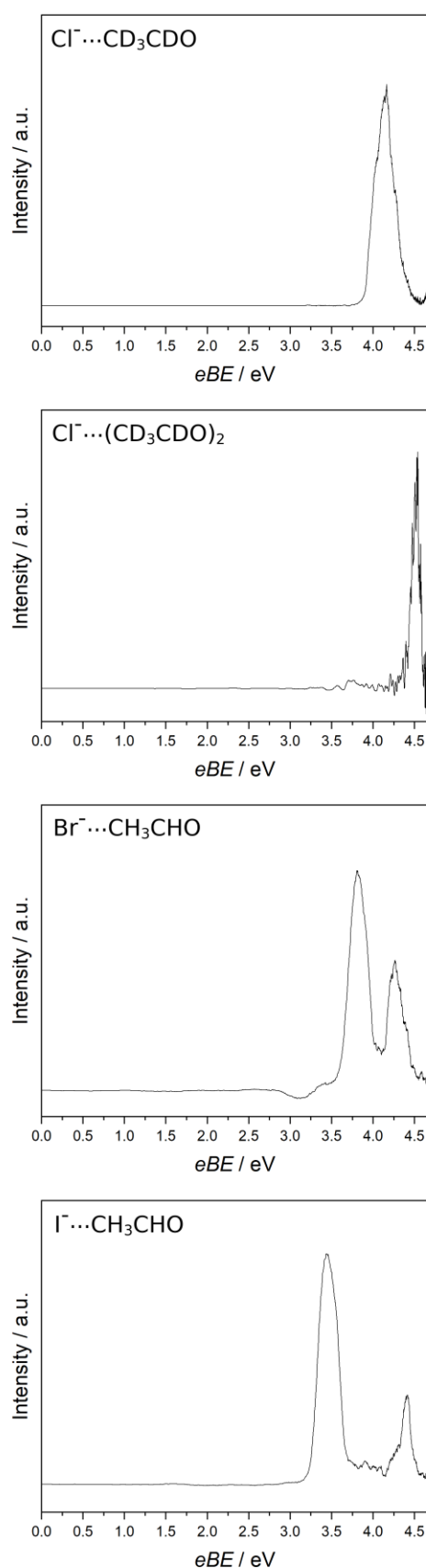


Figure 2. Anion photoelectron spectra of $\text{Cl}^- \cdots \text{CD}_3\text{CDO}$, $\text{Cl}^- \cdots (\text{CD}_3\text{CDO})_2$, $\text{Br}^- \cdots \text{CH}_3\text{CHO}$, and $\text{I}^- \cdots \text{CH}_3\text{CHO}$.

COMMUNICATION

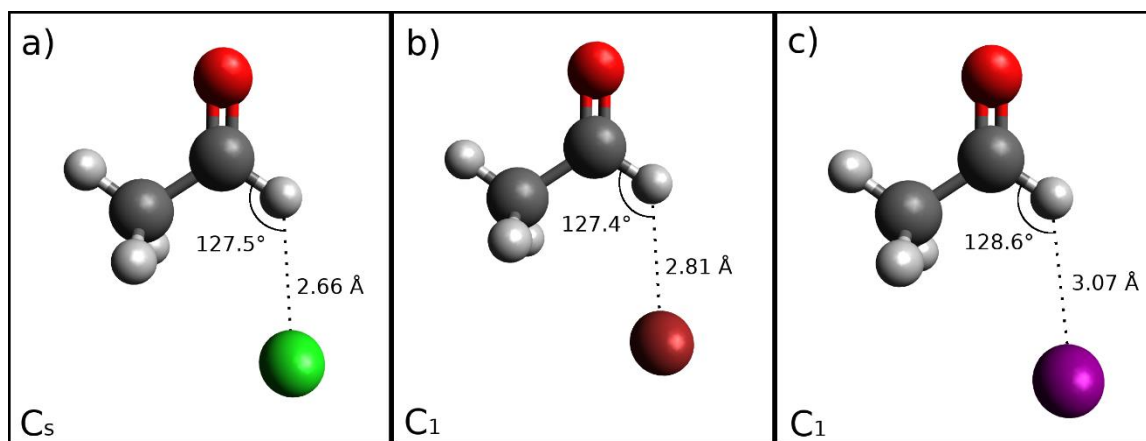


Figure 3. CCSD(T)/AVTZ optimized geometries of a) $\text{Cl}^- \cdots \text{CH}_3\text{CHO}$, b) $\text{Br}^- \cdots \text{CH}_3\text{CHO}$, and c) $\text{I}^- \cdots \text{CH}_3\text{CHO}$.

residing slightly out of the $\text{H}-\text{C}=\text{O}$ plane at 13.4° for the Br^- complex and 7.9° for the I^- complex. This suggests a more pronounced interaction with the rotatable methyl group of CH_3CHO . The smallest halide of the three, Cl^- , forms a complex with CH_3CHO in a fashion that retains the C_s symmetry of the molecule.

The nature of the symmetry change for the Br^- and I^- complexes presents itself as somewhat of a cautionary tale for computational investigations of CH_3CHO ; in that preliminary optimisations using MP2 resulted in C_s symmetry akin to $\text{Cl}^- \cdots \text{CH}_3\text{CHO}$. This infers that CCSD(T) is required to encapsulate the precise nature of intermolecular interactions on display for the singly solvated halide species.

However, in electronic energy, a C_s $\text{Br}^- \cdots \text{CH}_3\text{CHO}$ structure is only 0.02 kJ mol^{-1} less stable than the C_1 optimised geometry. This is even less for the C_s $\text{I}^- \cdots \text{CH}_3\text{CHO}$ transition structure relative to the C_1 ground state. Therefore, it is entirely possible that the vibrationally averaged structure is of C_s symmetry, similar to other systems explored by our group.^[9]

The dissociation energy, D_0 , of each anion complex is presented in Table 1, reducing from 51.6 kJ mol^{-1} for $\text{Cl}^- \cdots \text{CH}_3\text{CHO}$, to 50.8 kJ mol^{-1} for $\text{Br}^- \cdots \text{CH}_3\text{CHO}$, and 45.5 kJ mol^{-1} for $\text{I}^- \cdots \text{CH}_3\text{CHO}$. This decreasing trend can be rationalised in comparison to the E_{stab} values that align to the same pattern with respect to halide size.

The CCSD(T)/CBS detachment energies of Table 1, being the calculated difference in energy between the anion complexes and neutral counterparts at the same geometry, can be seen to have excellent agreement with the experimental results. This agreement justifies the level of theory utilised in this paper as appropriate, as well as allows the structure of halide anion complexes with CH_3CHO in the gas phase to be assigned as those in Figure 3.

It should be noted that the theoretical detachment energies were treated with a correction based on the zero-point energy (zpe) of the anion complex. A negligible difference in predicted detachment energy was observed between $\text{Cl}^- \cdots \text{CH}_3\text{CHO}$ and $\text{Cl}^- \cdots \text{CD}_3\text{CDO}$, although there was a difference of 0.03 eV between the predicted photodetachment of $\text{Cl}^- \cdots (\text{CH}_3\text{CHO})_2$ and $\text{Cl}^- \cdots (\text{CD}_3\text{CDO})_2$. This is further detailed in the Supporting Information.

The optimised geometry of $\text{Cl}^- \cdots (\text{CH}_3\text{CHO})_2$ in Figure 4 demonstrates the stepwise solvation of a Cl^- anion by CH_3CHO . There is a significant structural rearrangement relative to the

singly solvated $\text{Cl}^- \cdots \text{CH}_3\text{CHO}$ system, with the Cl^- anion tethered simultaneously to the formyl hydrogen of one CH_3CHO molecule at 2.84 \AA , and a methyl hydrogen of another CH_3CHO at 2.66 \AA

Table 1. Summary of experimental and theoretical energies of halide- $\text{CH}_3\text{CHO}/\text{CD}_3\text{CDO}$ systems. Unless stated otherwise, all theoretical energies are CCSD(T)/CBS values.

Complex	Experimental			Theoretical		
	${}^2\text{P}_{3/2}$ (eV)	${}^2\text{P}_{1/2}$ (eV)	E_{stab} (eV)	${}^2\text{P}_{3/2}$ (eV)	${}^2\text{P}_{1/2}$ (eV)	D_0 (kJ mol^{-1})
$\text{Cl}^- \cdots \text{CD}_3\text{CDO}$	4.16	-	0.55	4.16	4.27	51.6
$\text{Cl}^- \cdots (\text{CD}_3\text{CDO})_2$	4.54	-	0.93	4.55 ^[a]	4.66 ^[a]	-
$\text{Br}^- \cdots \text{CH}_3\text{CHO}$	3.82	4.27	0.48	3.84	4.30	50.8
$\text{I}^- \cdots \text{CH}_3\text{CHO}$	3.45	4.41	0.40	3.47	4.41	45.5

[a] From CCSD(T)/AVTZ single point energies.

Looking to Figure 4, it can be seen that the CH_3CHO molecules themselves have arranged in a 'ring-like' system so as to accommodate the Cl^- anion. One methyl hydrogen of a CH_3CHO molecule is aligned rather directionally with the carbonyl oxygen of the second CH_3CHO at a distance of 2.68 \AA and with an angle of 155.2° . This motif is reminiscent of the asymmetric solvation present in $\text{X}^- \cdots (\text{H}_2\text{O})_2$ anion complexes.^[11,12]

Due to the size of the system as well as the aforementioned difficulty with MP2 methods, a double-hybrid method in DSD-PBEP86^[44] was chosen for calculations involving $\text{Cl}^- \cdots (\text{CH}_3\text{CHO})_2$, having performed well with reference to the GMTKN55 database.^[45] Simulated electron detachment energies from CCSD(T)/AVTZ single point calculations were also found to be in excellent agreement with the experimental results. A deviation of only 0.01 eV was determined when comparing the experimental ${}^2\text{P}_{3/2}$ energy of $\text{Cl}^- \cdots (\text{CD}_3\text{CDO})_2$, 4.54 eV , relative to that computed, 4.55 eV . This infers that the double-hybrid approach has been an apt substitute for the full CCSD(T) treatment conducted on the singly solvated halides.

The current work bridges the gap between previous anion photoelectron spectroscopic studies involving halide anion complexes with simple carbonyl-containing molecules; namely, CH_2O and CH_3COCH_3 .^[37,38] As such, a summary of experimental E_{stab} values and computational D_0 energies has been compiled in

COMMUNICATION

Table 2. This table showcases energetic trends amongst the same halide species and differing carbonyl molecule, as well as differing halide anion with the same complexing solvent in the gas phase.

As is consistent with the trend observed in this work, E_{stab} numbers obey the increasing trend of $I^- < Br^- < Cl^-$ in both cases of CH_2O and CH_3COCH_3 . In the cases of Cl^- and Br^- , E_{stab} values increase in order of methyl substitution of the respective carbonyl molecule. That is to say, the trend is $CH_2O < CH_3CHO < CH_3COCH_3$. This is sensible as the number of hydrogen bonding opportunities increases across the series, allowing for a stronger interaction with the complexing halide.

This fact is certainly reflected when looking to the computational dissociation energies, D_0 , which follow the trend of $CH_2O < CH_3CHO < CH_3COCH_3$ for every halide. It is interesting to see that the experimental electron stabilisation energies follow the trend of $CH_3CHO < CH_2O < CH_3COCH_3$ for the I^- complexes.

This is perhaps rather unexpected given the D_0 of $I^- \cdots CH_2O$ has been reported as 43.2 kJ mol^{-1} ,^[37] while the D_0 of $I^- \cdots CH_3CHO$ is presented here as 45.5 kJ mol^{-1} . For comparison, $Cl^- \cdots CH_3CHO$ is more stable than $Cl^- \cdots CH_2O$ by 2.2 kJ mol^{-1} and incurs an E_{stab} increase of 0.04 eV . The unexpected deviation from the trend could then be rationalised in terms of stabilising effects on the $I^- \cdots CH_3CHO$ neutral potential energy surface.

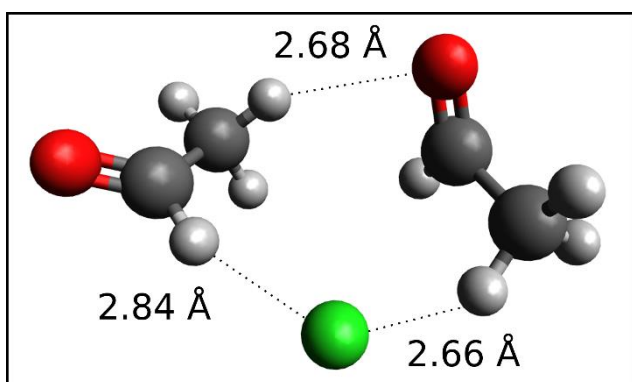


Figure 4. DSD-PBEP86/AVTZ optimised geometry of $Cl^- \cdots (CH_3CHO)_2$.

While the stability of the anion complex (D_0) has been established as an indicator of electron stabilisation (E_{stab}) previously,^[8-10] some effect on the neutral Franck-Condon surface may be resulting in a lower E_{stab} than expected for $I^- \cdots CH_3CHO$. Another way to delve further is to compare the predicted ${}^2P_{3/2}$ detachment energies of $I^- \cdots CH_2O$ from previous work and that of $I^- \cdots CH_3CHO$ reported here, in order to ascertain if the theory is consistent with the experimental observation.

Table 2. Comparison of E_{stab} and D_0 energies between halide complexes with CH_2O , CH_3CHO , and CH_3COCH_3 .

Solvent Molecule	Cl^-		Br^-		I^-	
	E_{stab} (eV)	D_0 (kJ mol^{-1})	E_{stab} (eV)	D_0 (kJ mol^{-1})	E_{stab} (eV)	D_0 (kJ mol^{-1})
CH_2O ^[37]	0.51	49.4	0.42	46.0	0.41	43.2
CH_3CHO ^{[a][b]}	0.55	51.6	0.48	50.8	0.40	45.5
CH_3COCH_3 ^[38]	0.62	56.9	0.54	56.2	0.44	50.2

[a] This work. [b] CD_3CDO was the solvent molecule for Cl^- .

In previous work, the ${}^2P_{3/2}$ photodetachment peak of $I^- \cdots CH_2O$ is predicted at 3.46 eV from CCSD(T)/CBS calculations, corresponding to a $0.40 \text{ eV } E_{stab}$.^[37] In this work, the ${}^2P_{3/2}$ photodetachment of $I^- \cdots CH_3CHO$ is reported as 3.47 eV from CCSD(T)/CBS results: a predicted E_{stab} of 0.41 eV . In short, the predicted detachment energies reverse the experimental ordering of E_{stab} values for $I^- \cdots CH_2O$ and $I^- \cdots CH_3CHO$. However, the predicted detachment energies for both species are only 0.01 eV apart, with the major conclusion drawn being the striking energetic similarity in comparing photodetachment from $I^- \cdots CH_2O$ and $I^- \cdots CH_3CHO$.

In summary, the anion photoelectron spectra of $Cl^- \cdots CD_3CDO$, $Cl^- \cdots (CD_3CDO)_2$, $Br^- \cdots CH_3CHO$, and $I^- \cdots CH_3CHO$ have been presented along with high level calculations of the anion complexes and predicted detachment energies. The $Cl^- \cdots CD_3CDO$ and $Cl^- \cdots (CD_3CDO)_2$ spectra are characterised by E_{stab} values, being the experimentally determined 'solvent shift', of 0.55 eV and 0.93 eV respectively. This corresponds to a 0.38 eV increase upon complexation with a second CD_3CDO molecule. $Br^- \cdots CH_3CHO$ and $I^- \cdots CH_3CHO$ were found to have electron stabilisation energies of 0.48 eV and 0.40 eV .

The CCSD(T)/AVTZ optimised geometries of $Cl^- \cdots CH_3CHO$, $Br^- \cdots CH_3CHO$, and $I^- \cdots CH_3CHO$ feature the halide anion appended to the formyl hydrogen of CH_3CHO and in-line with the electropositive end of the carbonyl bond. $Cl^- \cdots CH_3CHO$ was found to exhibit C_s symmetry while $Br^- \cdots CH_3CHO$ and $I^- \cdots CH_3CHO$ were found to be of C_1 symmetry, contradictory to calculations at lower levels of theory. These complexes are bound on the order of $45\text{--}52 \text{ kJ mol}^{-1}$ depending on the halide.

The DSD-PBEP86/AVTZ optimised geometry of $Cl^- \cdots (CH_3CHO)_2$ was found to form a 'ring-like' structure where the Cl^- anion interacts with a formyl hydrogen of one CH_3CHO molecule and a methyl hydrogen of the second CH_3CHO molecule, reflecting asymmetric solvation. Simulated detachment energies were found to be in excellent agreement with the experimental results. A comparison was made between the results of the current work and previous photoelectron spectroscopic studies involving CH_2O and CH_3COCH_3 , in order to catalog the fundamental energetics of halide anion complexes with archetypal carbonyl molecules.

Acknowledgements

This research was undertaken with the assistance of computational resources from the Pople high-performance computing cluster of the Faculty of Science at the University of Western Australia. The Australian Research Council is acknowledged for funding the laser installation under the LIEF scheme (LE110100093). The School of Molecular Sciences and the Faculty of Science are acknowledged for financial support. T.R.C. thanks the support of an Australian Government Research Training Program (RTP) scholarship, C.T.H. acknowledges the UWA Dean's Excellence in Science PhD Scholarship, and P.D.W. thanks the support of the Center for Materials Crystallography at Aarhus University in Denmark, funded by the Danish National Research Foundation (DNRF93). The Koutsantonis and Stewart groups at UWA are thanked for providing CH_3CHO for experiments.

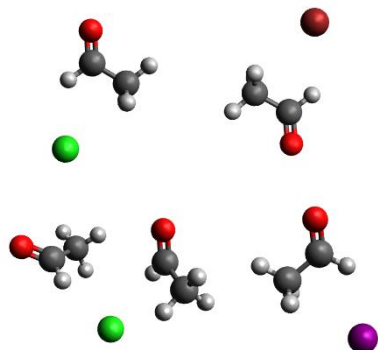
Keywords: noncovalent interactions • electronic structure • photoelectron spectroscopy • halides • ab initio calculations

COMMUNICATION

- [1] A. W. Castleman, Jr., K. H. Bowen, Jr., *J. Phys. Chem.* **1996**, *100*, 12911-12944.
- [2] D. M. Neumark, *J. Phys. Chem. A* **2008**, *112*, 13287-13301.
- [3] G. Markovich, R. Giniger, M. Levin, O. Cheshnovsky, *Z Phys D - Atoms, Molecules and Clusters* **1991**, *20*, 69-72.
- [4] G. Markovich, R. Giniger, M. Levin, O. Cheshnovsky, *J. Chem. Phys.* **1991**, *95*, 9416-9419.
- [5] G. Markovich, S. Pollack, R. Giniger, O. Cheshnovsky, *J. Chem. Phys.* **1994**, *101*, 9344-9353.
- [6] D. W. Arnold, S. E. Bradforth, E. H. Kim, D. M. Neumark, *J. Chem. Phys.* **1995**, *102*, 3510-3518.
- [7] R. Mabbs, E. Surber, A. Sanov, *J. Chem. Phys.* **2005**, *122*, 054308.
- [8] T. R. Corkish, C. T. Haakansson, A. J. McKinley, D. A. Wild, *J. Phys. Chem. Lett.* **2019**, *10*, 5338-5342.
- [9] C. T. Haakansson, T. R. Corkish, P. D. Watson, A. J. McKinley, D. A. Wild, *Chem. Phys. Lett.* **2020**, *761*, 138060.
- [10] P. D. Watson, A. J. McKinley, D. A. Wild, *J. Mol. Spectrosc.* **2020**, *372*, 111320.
- [11] P. Ayotte, S. B. Nielsen, G. H. Weddle, M. A. Johnson, S. S. Xantheas, *J. Phys. Chem. A* **1999**, *103*, 10665-10669.
- [12] P. Ayotte, G. H. Weddle, J. Kim, M. A. Johnson, *Chem Phys*, **1998**, *239*, 485-491.
- [13] J. M. Weber, J. A. Kelley, W. H. Robertson, M. A. Johnson, *J. Chem. Phys.* **2001**, *114*, 2698-2706.
- [14] E. M. Myshakin, K. D. Jordan, W. H. Robertson, G. H. Weddle, M. A. Johnson, *J. Chem. Phys.* **2003**, *118*, 4945-4953.
- [15] W. H. Robertson, K. Karapetian, P. Ayotte, K. D. Jordan, M. A. Johnson, *J. Chem. Phys.* **2002**, *116*, 4853-4857.
- [16] D. Grosjean, *Environ. Sci. Technol.* **1991**, *25*, 710-715.
- [17] E. Grosjean, E. L. Williams II, D. Grosjean, *Air Waste* **1993**, *43*, 469-474.
- [18] M. Possanzini, V. Di Palo, A. Cecinato, *Atmos. Environ.* **2002**, *36*, 3195-3201.
- [19] L. G. Anderson, J. A. Lanning, R. Barrell, J. Miyagishima, R. H. Jones, P. Wolfe, *Atmos. Environ.* **1996**, *30*, 2113-2123.
- [20] P. B. Shepson, A.-P. Sirju, J. F. Hopper, L. A. Barrie, V. Young, H. Niki, H. Dryfhout, *J. Geophys. Res.* **1996**, *101*, 21081-21089.
- [21] J. Sehested, L. K. Christensen, O. J. Nielsen, T. J. Wallington, *Int. J. Chem. Kinet.* **1998**, *30*, 913-921.
- [22] M. S. Taylor, S. A. Ivanic, G. P. F. Wood, C. J. Easton, G. B. Bacskay, L. Radom, *J. Phys. Chem. A*, **2009**, *113*, 11817-11832.
- [23] W. A. Payne, D. F. Nava, F. L. Nesbitt, L. J. Stief, *J. Phys. Chem.* **1990**, *94*, 7190-7193.
- [24] J. A. Beukes, B. D'Anna, V. Bakken, C. J. Nielsen, *Phys. Chem. Chem. Phys.* **2000**, *2*, 4049-4060.
- [25] M. T. Rayez, J. C. Rayez, E. Villenave, *Comput. Theor. Chem.* **2011**, *965*, 321-327.
- [26] H. Niki, P. D. Maker, C. M. Savage, L. P. Breitenbach, *J. Phys. Chem.* **1985**, *89*, 588-591.
- [27] G. S. Tyndall, J. J. Orlando, C. S. Kegley-Owen, T. J. Wallington, M. D. Hurley, *Int. J. Chem. Kinet.* **1999**, *31*, 776-784.
- [28] J. D. Smith, J. D. DeSain, C. A. Taatjes, *Chem. Phys. Lett.* **2002**, *366*, 417-425.
- [29] P. W. Seakins, J. J. Orlando, G. S. Tyndall, *Phys. Chem. Chem. Phys.* **2004**, *6*, 2224-2229.
- [30] C. S. Kegley-Owen, G. S. Tyndall, J. J. Orlando, A. Fried, *Int. J. Chem. Kinet.* **1999**, *31*, 766-775.
- [31] A. O. Hui, M. Okumura, S. P. Sander, *J. Phys. Chem. A*, **2019**, *123*, 4964-4972.
- [32] M. Bartels, K. Hoyermann, U. Lange, *Ber. Bunsenges. Phys. Chem.* **1989**, *93*, 423-427.
- [33] I. Szilágyi, K. Imrik, S. Dóbe, T. Bérces, *Ber. Bunsenges. Phys. Chem.* **1998**, *102*, 79-84.
- [34] H. Niki, P. D. Maker, C. M. Savage, L. P. Breitenbach, *Int. J. Chem. Kinet.* **1985**, *17*, 525-534.
- [35] T. S. A. Islam, R. M. Marshall, S. W. Benson, *Int. J. Chem. Kinet.* **1984**, *16*, 1161-1166.
- [36] B. Ramacher, J. J. Orlando, G. S. Tyndall, *Int. J. Chem. Kinet.* **2000**, *32*, 460-465.
- [37] T. R. Corkish, C. T. Haakansson, P. D. Watson, A. J. McKinley, D. A. Wild, *ChemPhysChem* **2021**, *22*, 69-75.
- [38] T. R. Corkish, D. B. 't Hart, P. D. Watson, A. J. McKinley, D. A. Wild, *J. Mol. Spectrosc.* **2019**, *364*, 111178.
- [39] O. H. Cheshnovsky, S. H. Yang, C. L. Pettiette, M. J. Craycraft, R. E. Smalley, *Rev. Sci. Instrum.* **1987**, *58*, 2131-2137.
- [40] R. A. Kendall, T. H. Dunning Jr, R. J. Harrison, *J. Chem. Phys.* **1992**, *96*, 6796-6806.
- [41] T. H. Dunning Jr, K. A. Peterson, A. K. Wilson, *J. Chem. Phys.* **2001**, *114*, 9244-9253.
- [42] K. A. Peterson, D. Figgen, E. Goll, H. Stoll, M. Dolg, *J. Chem. Phys.* **2003**, *119*, 11113.
- [43] K. A. Peterson, B. C. Shepler, D. Figgen, H. Stoll, *J. Phys. Chem. A* **2006**, *110*, 13877.
- [44] S. Kozuch, J. M. L. Martin, *Phys. Chem. Chem. Phys.* **2011**, *13*, 20104-20107.
- [45] L. Goerigk, A. Hansen, C. Bauer, S. Ehrlich, A. Najibi, S. Grimme, *Phys. Chem. Chem. Phys.* **2017**, *19*, 32184-32215.

COMMUNICATION

Entry for the Table of Contents



Fundamental ion solvation in the gas phase has been investigated via noncovalent complexes consisting of halide anions and CH_3CHO and CD_3CDO . This study delves into the interactions between halide anions and small carbonyl-containing molecules, uncovering molecular structures and observed electronic trends.

Institute and/or researcher Twitter usernames: @SMS_UWA
@DrDunk_UWA @timcorkish @laser_watson